ORIGINAL RESEARCH

Reduced Cortical Folding in Mental Retardation

Y. Zhang
Y. Zhou
C. Yu
L. Lin
C. Li
T. Jiang

BACKGROUND AND PURPOSE: MR is a developmental disorder associated with impaired cognitive functioning and deficits in adaptive behavior. With a 2D region of interest–based GI, a preliminary study reported significantly reduced gyrification in the prefrontal lobe in MR. The purpose of this study was to further investigate the abnormalities of cortical gyrification in MR and to explore the possible causes of these abnormalities.

MATERIALS AND METHODS: Thirteen patients with MR and 26 demographically matched healthy controls were included in this study. A 3D surface-based lGI was calculated as a measure to quantify gyrification. Then vertex-by-vertex contrasts of lGI were performed between patients with MR and healthy controls.

RESULTS: Statistical analysis showed that patients with MR had significantly reduced lGI in multiple brain regions compared with healthy controls. These regions include the lateral and medial prefrontal cortices, the right superior temporal gyrus, the left superior parietal lobe, the bilateral insular and adjacent cortices, and the visual and motor cortices.

CONCLUSIONS: The observed abnormal pattern of cortical gyrification revealed by significant reduction of lGI in multiple brain regions might reflect the developmental disturbance in intracortical organization and cortical connectivities in MR.

ABBREVIATIONS: A-GI = automated gyrification index; FA = fractional anisotropy; FSIQ = full scale intelligence quotient; GI = gyrification index; GLM = general linear model; ID = identification; IQ = intelligence quotient; lGI = local gyrification index; MR = mental retardation; RFT = random field theory

MR, also called developmental delay or mental delay, is a developmental disorder characterized by subaverage cognitive functioning and deficits in adaptive behaviors. The pathophysiologic basis underlying this disorder is still not fully understood. However, accumulating evidence has shown that MR is primarily due to deficiencies in neuronal network connectivity.[1-4] This opinion is supported by abnormalities in dendritic spine lengths and shapes in multiple brain regions.[5,6] Additionally, abnormalities in white matter connectivity revealed by disrupted white matter integrity have also been reported.[7,8]

Cortical folding, which appears in humans in the fifth fetal month and continues its development into the first postnatal year,[9] is thought to reflect not only corticocortical connectivity[10] but also optimal intracortical organization, with the most axonal connections in the least possible volume.[11] Many researchers have shown that abnormal patterns of cortical gyrification have been associated with cognitive-behavioral deficits among individuals with schizophrenia, developmental language disorders, and dyslexia[12-15]; however, few studies have been performed on cortical gyrification in MR, given its cognitive impairment. Using A-GI, a region-of-interest study reported that patients with MR have reduced gyrification in the prefrontal lobe compared with healthy controls.[16] Because studies have shown that MR involves alterations in multiple brain regions,[5,7,8] it is necessary to detect brain areas with abnormal cortical gyrification in MR by using a whole-brain analysis, which contributes to understanding the neuropathology of this disorder.

Several measures have been proposed to investigate the pattern of gyrification in the cerebral cortex. The GI,[17] a most widely used measure of gyrification, is defined as the ratio of the length of the pial perimeter of the cortex to the length of the outer perimeter on coronal sections (Fig 1). Formally

$$GI = \frac{\sum_{i=1}^{N} P_P^i}{\sum_{i=1}^{N} P_O^i},$$

where P_P^i is the pial cortical perimeter of section i and P_O^i is the outer perimeter of section i. However, this method is rater-dependent and cannot localize the exact regions with abnormal cortical gyrification. Another measure of gyrification is A-GI.[16] Although this method is automatic and does not need extra intervention, it still cannot localize specific regions with abnormal cortical gyrification.

Recently, curvature and functions of curvature have been used to analyze the developing brain from preterm to adult.[18] However, curvature-based approaches are highly dependent on surface configuration and are sensitive to noise. The lGI,[19] a 3D extension of the GI, is a newly developed automated

Received August 30, 2009; accepted after revision November 3.

From the Department of Mathematics (Y. Zhang, L.L., C.L.), Zhejiang University, Hangzhou, P. R. China; National Laboratory of Pattern Recognition (Y. Zhang, Y. Zhou, L.L., C.L., T.J.), Institute of Automation, and Center for Social and Economic Behavior (Y. Zhou), Institute of Psychology, Chinese Academy of Sciences, Beijing, P. R. China; and Department of Radiology (C.Y.), Tianjin Medical University General Hospital, Tianjin, P. R. China

Yuanchao Zhang, Yuan Zhou, and Chunshui Yu contributed equally to this work.

This work was supported by the National Key Basic Research and Development Program (973), grant 2007CB512305; the Natural Science Foundation of China, grant 30730035; and the Program for New Century Excellent Talents in University, grant NCET-07-0568. This work also received support from the Open Project Program of the National Laboratory of Pattern Recognition.

Please address correspondence to Tianzi Jiang, MD, National Laboratory of Pattern Recognition, Institute of Automation, Chinese Academy of Sciences, Beijing 100190, P. R. China; e-mail: jiangtz@nlpr.ia.ac.cn

DOI 10.3174/ajnr.A1984

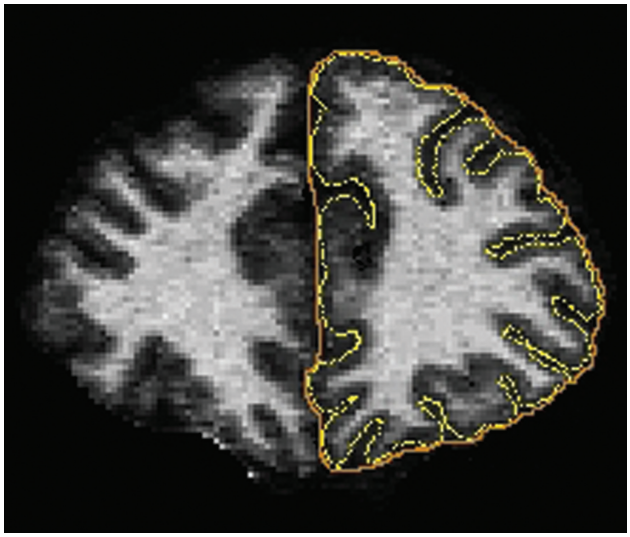

Fig 1. Schematic illustration of the GI defined as the ratio of the length of the pial perimeter (in yellow) of the cortex to the length of the outer perimeter (in orange) on coronal sections.

method for locating regionally specific changes in gyrification. This measure is able to quantify the amount of cortical surface invaginated in the sulci and measure the spatial frequency of cortical gyrification and the depth of the sulci. Compared with curvature-based approaches, the lGI method is less easily affected by noise in the surface configuration. The measure lGI has been successfully used to assess gyrification of the 22q11 Deletion Syndrome and major depressive disorder.[19-21] In this study, we used this measure to investigate gyrification abnormalities in MR. We contrasted the lGI between healthy controls and patients with MR by using a surface-based GLM tool to map group contrasts on a vertex-by-vertex basis. On the basis of previous studies,[5,7,8,16] we hypothesized that patients with MR would exhibit reductions in lGI in multiple brain regions, including the prefrontal lobe.

Materials and Methods

Subjects

All subjects of this study were chosen from those who participated in a study by Yu et al.[8] The 15 patients with idiopathic MR are described in detail by Yu et al, and 2 of them were excluded due to segmentation errors. In brief, the patients with MR were recruited from Beijing Huiling Community Service for People with Disabilities and Beijing Lizhi Recovery Center for People with Disabilities. All patients were diagnosed by an experienced psychiatrist according to the *Diagnostic and Statistical Manual of Mental Disorders* criteria for MR: 1) IQ of approximately 70 or below on an individually administered IQ test; 2) at least 2 affected areas: communication, self-care, home living, social/interpersonal skills, use of community resources, self-direction, functional academic skills, work, leisure, health, and safety; and 3) onset before 18 years of age. Exclusion criteria were prenatal events (such as congenital infections, prolonged maternal fever in the first trimester, exposure to anticonvulsants or alcohol, and untreated maternal phenylketonuria), notable dysmorphology, near-drowning, traumatic brain injury, phenylketonuria, hypothyroidism, and disorders known to be associated with MR, such as neurofibromatosis and tuberous sclerosis. Patients with visible brain lesions on conventional MR images were also excluded from this study. For comparison with the 13 subjects with MR (8 men and 5 women; mean age, 22.6 ± 2.3 years), 26 age- and sex-matched healthy subjects were included (16 men and 10 women; mean age, 23.4 ± 4.6 years). FSIQ score was measured by means of the Chinese Revised Wechsler Adult Intelligence Scale. The FSIQ was 50.0 ± 10.0 with a range of 33–63 for patients with MR and 108.1 ± 8.6 with a range of 91–120 for healthy controls.

MR Imaging Data Acquisition

3D structural MR imaging scans were obtained on a 3T scanner (Magnetom Trio; Siemens, Erlangen, Germany) with magnetization-prepared rapid acquisition of gradient echo imaging. Detailed scanning parameters were as follows: TR = 2000 ms, TE = 2.6 ms, section thickness = 1 mm, no gaps, flip angle = 9°, matrix = 256 × 224, FOV = 256 × 224 mm^2, 1 × 1 mm^2 in-plane resolution.

Preprocessing

Each scan was processed by using FreeSurfer[22,23] (http://surfer.nmr.mgh.harvard.edu) with its volume and surface pipeline. Starting from the segmentation of white matter and tessellation of the gray/white matter boundary, we obtained an initial surface after automated topologic correction. This surface was used as the initial shape for the deformable model that was used to reconstruct the pial surface. After obtaining the pial surface, one can obtain a cortical map of lGIs in 3 steps.[19] First, an outer surface can be obtained by triangulating the outer hull, which tightly wraps the pial surface. Second, the lGIs were calculated for vertices on the outer surface by using following formula:

$$lGI\,|_{3-D}^{Outer}(v_i) = \frac{\sum_{\forall\, j \in S'(v_i,\, r)} A_p^j}{\sum_{\forall\, j \in S(v_i,\, r)} A_O^j}, \forall\, v_i \in S_o,$$

where $S(v_i, r)$ is a sphere centered on vertex v_i of the outer surface S_O with a radius r, A_O^j is the area of the face j of S_O that lies inside the contour delineated by the intersection of the outer surface S_O with the sphere $S(v_i, r)$, and A_p^j is the area of the face j of the pial surface that lies inside the contour $S'(v_i, r)$ delineated by the vertices of the pial surface that are closest to each vertex of the outer contour. Third, the lGI for each vertex on the pial surface was obtained by propagating the lGI values from the outer surface mesh to the pial surface mesh according to its prior involvement in the whole computational process. Mathematically

$$lGI\,|_{3-D}^{Pial}(v_j) = \frac{\sum_{\forall\, v_j,\, v_i \in S'(v_i,\, r)} lGI\,|_{3-D}^{Outer}(v_i) \cdot \left[1 - \frac{1}{d(v_j,\, X(v_i))}\right]}{\sum_{\forall\, v_j,\, v_i \in S'(v_i,\, r)} \left[1 - \frac{1}{d(v_j,\, X(v_i))}\right]}, \forall\, v_j \in S_p,$$

where $d(v_j, X(v_i))$ is the distance between v_j and the normal axis X to the outer surface at the vertex v_i.

The establishment of a vertex correspondence across subjects in a standard surface-based coordinate system was required to compare the lGIs vertex by vertex. Surface-based registration[24] was used to build an average template based on cortical surfaces from all 39 subjects. All of the individual reconstructed cortical surfaces were aligned to the template. Then the lGI data were resampled for each subject. Before statistical analysis, a heat kernel of 10-mm width was used to

Regions with reduced lGI in patients with MR		
Cluster ID	Anatomic Regions	Cluster Size
1	Left insular and its adjacent frontal and temporal cortices	9737 vertices
2	Right insular and its adjacent frontal and temporal cortices	8691 vertices
3	Left primary visual cortices and their associated cortices	1952 vertices
4	Right primary visual cortices and their associated cortices	2308 vertices
5	Left medial prefrontal cortex	1665 vertices
6	Right medial prefrontal cortex	2361 vertices
7	Left precentral gyrus	956 vertices
8	Right precentral gyrus	115 vertices
9	Right orbital frontal cortex	677 vertices
10	Right orbital frontal cortex	292 vertices
11	Right superior temporal gyrus	525 vertices
12	Left superior parietal lobe	290 vertices

smooth the lGI maps to increase the signal intensity–to-noise ratio and to improve the ability to detect morphometric variations.

Statistical Analyses

Vertex-by-vertex contrasts of lGI were performed for healthy controls versus patients with MR by using the SurfStat package (http://www.math.mcgill.ca/keith/surfstat). Specifically, each contrast was entered into a vertex-by-vertex GLM, including diagnosis, sex, and exact age as covariates. Subsequently, a corrected vertex-wise *P* value was obtained by using RFT.[25] The level of significance for vertices was set at a conservative surface-wide $P < .05$ after multiple-comparison correction. Only clusters with a minimum of 100 vertices were reported.

Results

Compared with healthy controls, only decreased lGI was observed in multiple brain regions in MR. We found 12 regions of difference with thresholds of $P < .05$ (corrected) and cluster sizes of ≥100 vertices. These regions included the bilateral insular and their adjacent frontal and temporal cortices, the bilateral medial prefrontal cortices, the bilateral primary visual cortices and their association cortices, the bilateral precentral gyri, the right orbital frontal cortex (2 clusters), the right superior temporal gyrus, and the left superior parietal lobe (Table). For visualization, regions of difference were projected onto the pial and inflated surfaces of the average template, respectively (Fig 2).

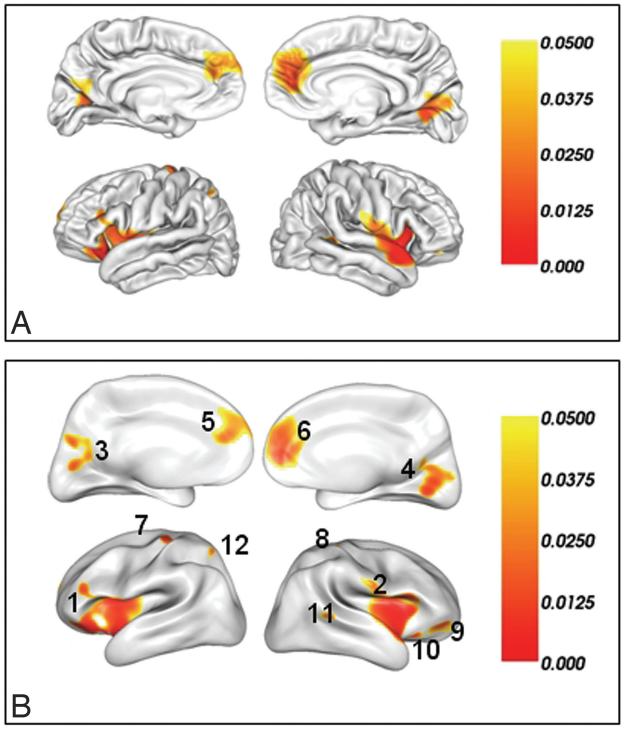

Fig 2. Brain regions of significantly reduced lGI in patients with MR compared with well-matched healthy subjects after a correction for multiple comparisons ($P < .05$, the vertex-based RFT correction) on the pial surface (*A*) and the inflated surface (*B*). The color bar indicates the vertex-wise *P* value after the correction for multiple comparisons. The integers in (*B*) are the cluster IDs corresponding to those of the Table.

Discussion

In this study, a whole-brain analysis of cortical gyrification was performed in patients with MR and demographically matched healthy controls. Unlike traditional region of interest−based methods, which need, a priori, to define the region of interest and limit the identification of changes elsewhere in the cortex, the surface-based lGI method does not need a priori definition and is able to detect localized abnormalities in gyrification. In addition, the lGI method is an automated one, which does not introduce user bias and does not need labor-intensive manual delineations. However, it needs high amounts of time to compute the lGIs for all the vertices on the pial surface. Using this measure, we detected significantly reduced lGI in the bilateral medial prefrontal cortices and the right orbital frontal cortex. These results are consistent with a previous region-of-interest study, which revealed decreased gyrification in the prefrontal cortex in MR.[16] Moreover, we also detected reduced lGI in the bilateral insular and adjacent frontal and temporal cortices, the bilateral primary visual cortices and their associated cortices, the bilateral precentral gyri, the right superior temporal gyrus, and the left superior parietal lobe. These abnormalities in cortical gyrification revealed by significant reduction of lGI may suggest a developmental disturbance in intracortical organization and cortical connectivities in MR.

There are several possible explanations for the observed abnormalities of cortical gyrification in the regions in MR. A mechanical model of brain convolutional development has been used to explain abnormalities in cortical folding during human brain development.[9] This model proposes that differential growth rates of cortical layers directly affect the degree of cortical convolutions. Indeed, several studies have observed developmental abnormalities in cortical layers in MR. For example, long thin tortuous dendritic spines with prominent heads and irregular dilations on apical dendrites of pyramidal

cells in layers III and V of the parieto-occipital neocortex and in the pyramidal layer of the allocortex have been reported in patients with fragile X syndrome.[26,27] In addition, Irwin et al[5] reported abnormal length and shape of dendritic spines in temporal and visual cortices of patients with fragile X syndrome. In the same study, higher attenuation of dendritic spines on distal segments of apical and basilar dendrites in both temporal and visual cortices has also been observed in patients with fragile X syndrome. Therefore, the abnormalities of cortical gyrification detected in MR might be caused by disorganization of the cortical architectures in these regions. An alternate theory to the mechanical model of gyrification suggests that changes in subcortical connections can lead to altered cortical folding patterns without changing the area of the cortical surface.[28] It has been known that cortical layer IV is a primary site for thalamocortical connections.[29] Moreover, abnormalities in subcortical structure such as fragile X syndrome have been reported in MR.[30-32] Abnormalities in subcortical structure might also be a possible cause of the abnormal cortical folding pattern in MR.

Another tension-based model of cortical morphogenesis proposes that the mechanical tension along axons is the driving force for cortical folding.[10] In fact, increasing research on MR has reported abnormalities in the corpus callosum,[33-35] which is the major white matter tract connecting the left and the right cerebral hemispheres. Diffusion tensor imaging also showed that patients with MR have significantly lower FA than healthy controls in the corpus callosum, uncinate fasciculus, optic radiation, and corticospinal tract.[8] In addition, lower FA values in the white matter in the frontostriatal pathways and in the parietal sensory-motor tracts have also been reported in MR, as in fragile X syndrome.[7] According to the above tension-based model of cortical morphogenesis, the gyral abnormalities might be due to the aberrant cortical connectivity caused by white matter abnormalities in these regions.

On the basis of the above discussion, both models could explain the gyral abnormalities in MR. However, which model plays a leading role in causing the gyrification changes remains beyond guarded conclusions. It is likely that the above models might not be mutually exclusive and might be coexistent; this possibility would explain the gyral abnormalities in MR. To obtain a better understanding of the pathogenesis of MR, one must explore the causes and underlying mechanisms of the abnormal cortical folding pattern. For years, it has been known that MR may result from both genetic and harmful environmental factors during the developmental process. Both of these factors may have an effect on the pattern of cortical folding.[36,37] Although some environmental factors that are often involved in MR have been excluded in this study, it is still possible that other harmful environmental factors, such as hypoxia, might have an effect on the cortical folding pattern. More important, genetic factors may play a critical role in abnormal cortical development. In fact, mutations in some genes implicated in MR, such as *fragile X mental retardation 1 gene*, *oligophrenin 1*, *p21-activated kinase*, and *rho guanine nucleotide exchange factor 6*, have been found to directly and indirectly affect intracortical architecture and cortical connectivities.[1,4,5,7] Future studies will need to discriminate the role of specific genetic and/or environmental factors in the development of the abnormal cortical folding pattern in MR by using samples with higher homogeneity or animal experiments.

Conclusions

We found significant reduction of lGI in multiple brain regions in patients with MR compared with healthy controls. The observed abnormalities of cortical gyrification might be the reflection of developmental abnormalities in both intracortical architecture and cortical connectivities in MR.

Acknowledgments

We thank Roberto Toro, Marie Schaer, Bing Liu, and Bing Hou for their useful suggestions and Yongfu Hao for his help with the artwork.

References

1. Chechlacz M, Gleeson JG. **Is mental retardation a defect of synapse structure and function?** *Pediatr Neurol* 2003;29:11–17
2. Dierssen M, Ramakers GJ. **Dendritic pathology in mental retardation: from molecular genetics to neurobiology.** *Genes Brain Behav* 2006;5(suppl 2):48–60
3. Ramakers GJ. **Rho proteins and the cellular mechanisms of mental retardation.** *Am J Med Genet* 2000;94:367–71
4. Ramakers GJ. **Rho proteins, mental retardation and the cellular basis of cognition.** *Trends Neurosci* 2002;25:191–99
5. Irwin SA, Patel B, Idupulapati M, et al. **Abnormal dendritic spine characteristics in the temporal and visual cortices of patients with fragile-X syndrome: a quantitative examination.** *Am J Med Genet* 2001;98:161–67
6. Kaufmann WE, Moser HW. **Dendritic anomalies in disorders associated with mental retardation.** *Cereb Cortex* 2000;10:981–91
7. Barnea-Goraly N, Eliez S, Hedeus M, et al. **White matter tract alterations in fragile X syndrome: preliminary evidence from diffusion tensor imaging.** *Am J Med Genet B Neuropsychiatr Genet* 2003;118B:81–88
8. Yu C, Li J, Liu Y, et al. **White matter tract integrity and intelligence in patients with mental retardation and healthy adults.** *Neuroimage* 2008;40:1533–41
9. Caviness VS Jr. **Mechanical model of brain convolutional development.** *Science* 1975;189:18–21
10. Van Essen DC. **A tension-based theory of morphogenesis and compact wiring in the central nervous system.** *Nature* 1997;385:313–18
11. Klyachko VA, Stevens CF. **Connectivity optimization and the positioning of cortical areas.** *Proc Natl Acad Sci U S A* 2003;100:7937–41
12. Sallet PC, Elkis H, Alves TM, et al. **Reduced cortical folding in schizophrenia: an MRI morphometric study.** *Am J Psychiatry* 2003;160:1606–13
13. Casanova MF, Araque J, Giedd J, et al. **Reduced brain size and gyrification in the brains of dyslexic patients.** *J Child Neurol* 2004;19:275–81
14. Harris JM, Yates S, Miller P, et al. **Gyrification in first-episode schizophrenia: a morphometric study.** *Biol Psychiatry* 2004;55:141–47
15. Jackson T, Plante E. **Gyral morphology in the posterior Sylvian region in families affected by developmental language disorder.** *Neuropsychol Rev* 1996;6:81–94
16. Bonnici HM, William T, Moorhead J, et al. **Pre-frontal lobe gyrification index in schizophrenia, mental retardation and comorbid groups: an automated study.** *Neuroimage* 2007;35:648–54
17. Zilles K, Armstrong E, Schleicher A, et al. **The human pattern of gyrification in the cerebral cortex.** *Anat Embryol* (*Berl*) 1988;179:173–79
18. Pienaar R, Fischl B, Caviness V, et al. **A methodology for analyzing curvature in the developing brain from preterm to adult.** *Int J Imaging Syst Technol* 2008;18:42–68
19. Schaer M, Cuadra MB, Tamarit L, et al. **A surface-based approach to quantify local cortical gyrification.** *IEEE Trans Med Imaging* 2008;27:161–70
20. Schaer M, Glaser B, Cuadra MB, et al. **Congenital heart disease affects local gyrification in 22q11.2 deletion syndrome.** *Dev Med Child Neurol* 2009;51:746–53
21. Zhang Y, Yu C, Zhou Y, et al. **Decreased gyrification in major depressive disorder.** *Neuroreport* 2009;20:378–80
22. Dale AM, Fischl B, Sereno MI. **Cortical surface-based analysis. I. Segmentation and surface reconstruction.** *Neuroimage* 1999;9:179–94
23. Fischl B, Sereno MI, Dale AM. **Cortical surface-based analysis. II: Inflation, flattening, and a surface-based coordinate system.** *Neuroimage* 1999;9:195–207
24. Fischl B, Sereno MI, Tootell RB, et al. **High-resolution intersubject averaging and a coordinate system for the cortical surface.** *Hum Brain Mapp* 1999;8:272–84

25. Worsley KJ, Andermann M, Koulis T, et al. **Detecting changes in nonisotropic images.** *Hum Brain Mapp* 1999;8:98–101
26. Rudelli RD, Brown WT, Wisniewski K, et al. **Adult fragile X syndrome.** *Acta Neuropathol* 1985;67:289–95
27. Wisniewski KE, Segan SM, Miezejeski CM, et al. **The Fra(X) syndrome: neurological, electrophysiological, and neuropathological abnormalities.** *Am J Med Genet* 1991;38:476–80
28. Kostovic I, Rakic P. **Developmental history of the transient subplate zone in the visual and somatosensory cortex of the macaque monkey and human brain.** *J Comp Neurol* 1990;297:441–70
29. Kostovic I, Judas M. **Correlation between the sequential ingrowth of afferents and transient patterns of cortical lamination in preterm infants.** *Anat Rec* 2002;267:1–6
30. Eliez S, Blasey CM, Freund LS, et al. **Brain anatomy, gender and IQ in children and adolescents with fragile X syndrome.** *Brain* 2001;124(pt 8):1610–18
31. Hoeft F, Lightbody AA, Hazlett HC, et al. **Morphometric spatial patterns differentiating boys with fragile X syndrome, typically developing boys, and developmentally delayed boys aged 1 to 3 years.** *Arch Gen Psychiatry* 2008;65:1087–97
32. Lee AD, Leow AD, Lu A, et al. **3D pattern of brain abnormalities in fragile X syndrome visualized using tensor-based morphometry.** *Neuroimage* 2007;34:924–38. Epub 2006 Dec 8
33. Widjaja E, Nilsson D, Blaser S, et al. **White matter abnormalities in children with idiopathic developmental delay.** *Acta Radiol* 2008;49:589–95
34. Soto-Ares G, Joyes B, Lemaitre MP, et al. **MRI in children with mental retardation.** *Pediatr Radiol* 2003;33:334–45
35. Spencer MD, Gibson RJ, Moorhead TW, et al. **Qualitative assessment of brain anomalies in adolescents with mental retardation.** *AJNR Am J Neuroradiol* 2005;26:2691–97
36. Piao X, Hill RS, Bodell A, et al. **G protein-coupled receptor-dependent development of human frontal cortex.** *Science* 2004;303:2033–36
37. Rees S, Stringer M, Just Y, et al. **The vulnerability of the fetal sheep brain to hypoxemia at mid-gestation.** *Brain Res Dev Brain Res* 1997;103:103–18